

Original article

Experimental Studies of the Long-Wave Barotropic and Baroclinic Fluctuations in the Shallow Bays and Gulfs of Marginal Seas (Using the Example of Posyet Bay in the Sea of Japan)

V. V. Novotryasov ^{1, ✉}, G. V. Shevchenko ²

¹ V. I. Il'ichev Pacific Oceanological Institute, Far Eastern Branch of Russian Academy of Sciences,
Vladivostok, Russian Federation

² Institute of Marine Geology and Geophysics, Far Eastern Branch of Russian Academy of Sciences,
Yuzhno-Sakhalinsk, Russian Federation

✉ vadimnov@poi.dvo.ru

Abstract

Purpose. The purpose of the work is to study the spectral composition and identify the mechanisms of formation of submesoscale and mesoscale variability of hydrological parameters (sea level, temperature, and bottom pressure) in the Posyet Bay coastal waters during the maximum development of the seasonal pycnocline.

Methods and Results. The internal gravity waves (IGW) were recorded using the measurement data on sea level (level gauge), temperature in the pycnocline layer and bottom pressure, as well as the methods for isolating its baroclinic component. Standard methods of spectral analysis and filtration, as well as analytical modeling were applied for assessing the periods of background fluctuations of the bay. It has been established that submesoscale variability is formed by the zero and higher modes of the bay seiche oscillations, as well as the offshore seiches induced by the Poincaré waves. The spectra of temperature and baroclinic pressure have a similar structure, and their decrease in the high-frequency range is described by the law $\sim \omega^{-3}$. In the mesoscale range (periods are from hours to minutes), the oscillations at tidal frequencies (M_2 and its subharmonics) and quasi-inertial oscillations are revealed. The presence of internal Kelvin waves has been proved, and the maxima in the pressure spectrum at the frequencies $\sim 1/16$ and $1/17 \text{ h}^{-1}$ are interpreted as the result of their Doppler shift in the coastal current.

Conclusions. The study has confirmed the assumption that the variability of hydrological parameters in the Posyet Bay is of a topographic nature and is formed by a set of resonant processes, including its own and forced seiches, as well as by internal waves exhibiting nonlinear properties. Recording of the baroclinic component of bottom pressure has proven to be an effective method for detecting internal Kelvin waves.

Keywords: Posyet Bay, sea shelf, sea level, seawater temperature, bottom pressure, seiches, offshore seiches, Kelvin internal waves

Acknowledgments: The study was carried out within the framework of the state assignment of the Pacific Oceanological Institute, FEB RAS (Project No. 1240-2210-0072-5).

For citation: Novotryasov, V.V. and Shevchenko, G.V., 2026. Experimental Studies of the Long-Wave Barotropic and Baroclinic Fluctuations in the Shallow Bays and Gulfs of Marginal Seas (Using the Example of Posyet Bay in the Sea of Japan). *Physical Oceanography*, 33(1), pp. 62-77.

© 2026, V. V. Novotryasov, G. V. Shevchenko

© 2026, Physical Oceanography

Introduction

Seiches are standing fluctuations of a fluid in enclosed or semi-enclosed areas [1], representing a typical example of a barotropic process. Studying this phenomenon in marine coastal waters is of great practical importance, as a sharp



intensification of seiches under certain conditions can lead to a short-term increase in the amplitudes of incoming waves of various origins. Primarily, this includes tsunami waves, whose typical periods are close to the resonant periods of most bays and inlets of the Russian Far East. Seiches can also amplify storm surges, which pose a serious threat to the population and coastal structures [2].

In addition to barotropic seiches, baroclinic long-wave fluctuations play a significant role in coastal water dynamics. These are periodic changes in hydrophysical parameters caused by long internal gravity waves (IGWs)¹ [3]. The wave processes they generate significantly influence mass and momentum transport, determining horizontal dispersion and vertical mixing, which are critical for biogeochemical processes in gulfs and bays [4, 5].

In semi-enclosed marine areas, such as gulfs and bays, resonant seiche oscillations (SOs) at the fundamental (zero) and subsequent mode frequencies make a defining contribution to the submesoscale and mesoscale variability of hydrophysical parameters, including sea level [6]. The mechanism for generating such SOs in these areas has several significant features. Seiches there are predominantly excited through the open boundary, meaning they are induced. A significant role in submesoscale sea level variability is played by oscillations induced by edge and radiated waves from the shelf zone adjacent to the bays.

One such semi-enclosed area is the Posyet Bay. Results from field studies of sea-level SOs in bays of this gulf have been published in [7, 8]. Numerical modeling of these processes in the specified bays was performed in [9]. However, the baroclinic oscillations of hydrological parameters in this bay and its adjacent bays, caused by IGWs, have not been previously investigated in a comprehensive manner. The present work aims to fill this gap through field research of both barotropic processes (using sea-level oscillations in the bay as an example) and baroclinic processes (using temperature and bottom pressure oscillations in the coastal waters of the bay as an example) in the Posyet Bay.

For this purpose, original measurement data were used: sea level data (from a custom-designed tide gauge installed on the coast at the entrance to the Vityaz Bay, in the northeastern part of the studied area), temperature data from the bay's coastal waters (from a submerged buoy station installed at the 35 m isobath in the coastal zone of the Gamov Peninsula), and bottom pressure data (from an ARV K-14 level recorder developed by SCTB EIIPA, Uglich, installed at the ~27 m isobath near the open boundary of the Vityaz Bay).

The present work is aimed at investigating the spectral composition of submesoscale oscillations and interpreting the features of mesoscale oscillations of sea level, bottom pressure, and temperature in the coastal waters of the Posyet Bay. To achieve this aim, the following tasks were addressed:

a) identification and analysis of the predominant frequencies (periods) in the spectra of oscillations of the specified parameters;

b) interpretation of the obtained spectra from the perspectives of seiche and radiated wave theory, as well as considering the possible influence of internal nonlinear gravity waves.

¹ Monin, A.S. and Kamenkovich, V.M., eds., 1978. *Physics of the Ocean* (in 2 Volumes). Moscow: Nauka, 455 p. (in Russian).

Description of the study area, data used, and processing methodology

Fig. 1 shows a bathymetric map of the Posyet Bay and its constituent inlets. The inset shows the Peter the Great Bay of the Sea of Japan. Topographic and bathymetric data were obtained from navigational charts ².

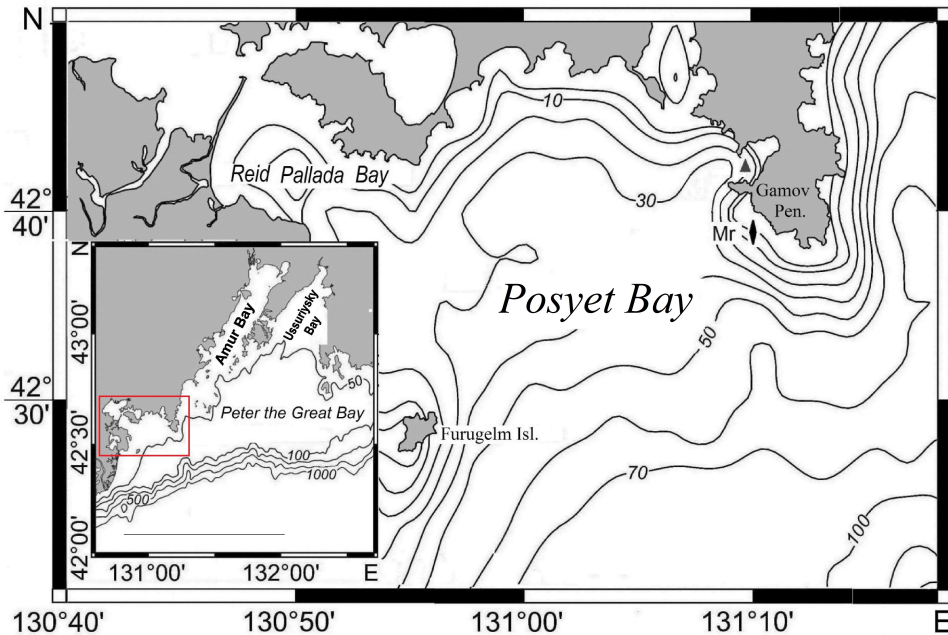


Fig. 1. Bathymetric map of the Posyet Bay and its constituent bays (the pressure sensor position is marked with a triangle, and the submerged buoy station with a diamond). The inset shows its position in the Peter the Great Bay (the Sea of Japan) outlined by a red rectangle

The spectral composition of sea level (ζ) fluctuations was investigated using measurement data from different years, obtained with a level gauge and a pressure sensor manufactured by SCTB EIPA. The sensor had an upper absolute pressure measurement limit (UPL), a submersion depth of 50 m, a resolution of 0.0008% of UPL, and a primary reduced error of $\pm 0.06\%$ of UPL. Baroclinic oscillations in the bay were studied using data on the baroclinic component of bottom pressure and coastal water temperature, obtained from a submerged buoy station (SBS) deployed on July 14, 2009, at the 35 m isobath.

The buoy station was equipped with an autonomous HOBO digital thermograph (Onset, USA) with an accuracy of $0.21\text{ }^{\circ}\text{C}$ in the range from 0 to $50\text{ }^{\circ}\text{C}$, a resolution of 0.02 at $25\text{ }^{\circ}\text{C}$, and a memory of 64 KB ($\sim 42,000$ 12-bit measurements). The thermograph was placed in the seasonal pycnocline layer 20 m above the bottom. Temperature recording at the station was conducted with a 1-minute sampling interval. The measurement duration exceeded 50 days.

² Ministry of Emergency Situations of Russia, 2003. [*Atlas of Peter the Great Bay and the Northwestern Coast of the Sea of Japan to Sokolovskaya Bay (for Small Vessels)*]. Vladivostok: KTOF Hydrographic Service, 10 p. (in Russian).

The spectral composition of sea level (ζ) fluctuations, temperature (T) fluctuations, and bottom pressure (p) fluctuations of marine waters in the bay was studied using methods of standard spectral analysis³ [10]. The original ζ , T , and p oscillations were separated into submesoscale and low-frequency background components using a Hamming filter with a 480-minute window. The background component was used to extract realizations in the submesoscale frequency range of $1/8$ – $1/256$ min^{-1} , which were calculated as the difference between the background and original realizations of sea level, temperature, and bottom pressure. The resulting time series of ζ , p , and T oscillations were used to calculate the spectral density of level oscillations (Sp_{ζ}), pressure fluctuations (Sp_{pp}), and temperature (Sp_T).

Results and discussion

Frequency composition of submesoscale sea level fluctuations in the Posyet Bay

Sea level measurement data from the entrance to the Vityaz Bay, obtained in 2001 and 2003 using a custom-designed tide gauge (accuracy 0.5 cm), were used for the analysis. Recording was performed to an electronic data logger with internal flash memory. The signal sampling interval from the tide gauge was 7.5 minutes in 2001 and 1 minute in 2003.

The spectral structure of sea level fluctuations was studied using a two-week-long record obtained in August 2003. Its high-frequency component was used for the analysis. Fig. 2 shows the sea level oscillation spectrum normalized to its maximum value for August 2003 in the frequency ranges of $1/8$ – $1/2048$ min^{-1} (Fig. 2, *a*) and $1/8$ – $1/256$ min^{-1} (Fig. 2, *b*). The main spectral energy in Fig. 2, *a* is concentrated at low frequencies corresponding to periods of ~ 12.3 h ($1/740$ min^{-1}) and ~ 25.6 h ($1/1540$ min^{-1}), with a rapid spectral decay towards higher frequencies.

The spectrum of submesoscale sea level fluctuations, normalized to its maximum value occurring at period $T_0 \sim 48$ min, is characterized by a narrowband maximum at period T_0 and less intense broadband maxima at periods of ~ 93 , ~ 146 , and ~ 205 min (Fig. 2, *b*). Furthermore, in the period range from 10 to 40 min, maxima are observed at periods of ~ 18 , ~ 22 , ~ 25 , and ~ 28 min.

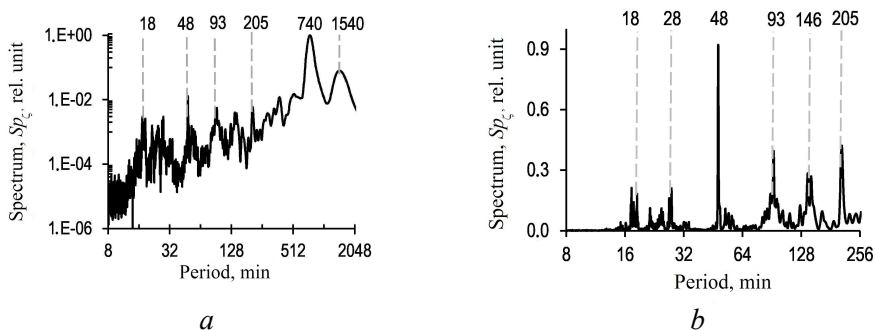


Fig. 2. Spectrum of sea-level oscillations (August 2003) in the frequency ranges $1/8$ – $1/2048$ min^{-1} (*a*) and $1/8$ – $1/256$ min^{-1} (*b*). Numbers above the peaks indicate periods in minutes

³ Dragan, Ya.P., Rozhkov, V.A. and Yavorskiy, I.N., 1987. [*Methods of Probabilistic Analysis of Rhythms in Oceanological Processes*]. Leningrad: Gidrometeoizdat, 319 p. (in Russian).

The stability of the spectral structure of sea level fluctuations in the bay was assessed using monthly records from the autumn period of 2001 (Fig. 3).

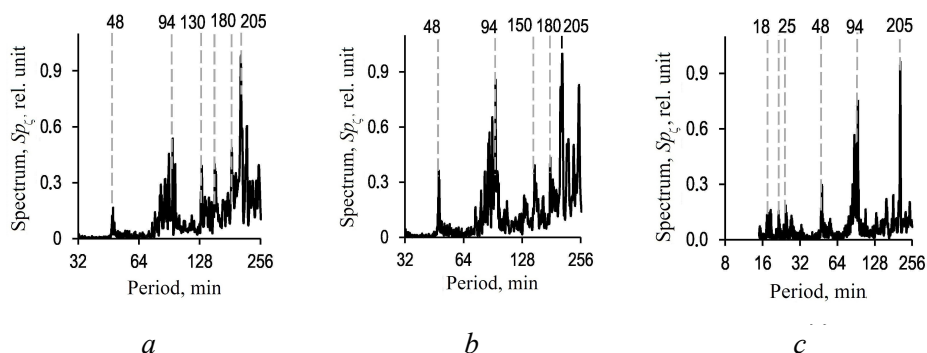


Fig. 3. Spectra of sea level fluctuations in September (a), October (b) and November (c), 2001

Here and elsewhere on the spectra, the period is plotted on the abscissa on a logarithmic scale. The spectra were calculated with a window length of 5760 data points (spectral resolution $\Delta\omega \cong 1.45 \cdot 10^{-4}$ rad/min) and 21 degrees of freedom.

The analysis revealed specific features of the presented spectra: first, stable narrowband maxima at frequencies of $1/48$, $1/94$, and $1/205$ min^{-1} ; second, broadband maxima at high frequencies of $1/18$, ..., $1/27$, $1/32$ min^{-1} , most pronounced in the September spectrum; and third, unstable broadband maxima at low frequencies of $1/109$, $1/130$, ..., $1/180$, and $1/208$ min^{-1} .

Thus, the spectral analysis of sea level fluctuations in the bay within the frequency range of $1/8$ – $1/256$ min^{-1} , based on records one month and two weeks long, revealed a stable characteristic spectral structure. This structure is characterized by three narrowband maxima, four broadband maxima, and several unstable broadband maxima.

Estimation of barotropic fluctuation periods on the shelf adjacent to the Posyet Bay and in the Amursky and Ussuriysky gulfs

Estimates of sea level seiche oscillation (SO) periods for the Posyet Bay were previously obtained in [11] based on a model area approximating its waters. The model area had an open boundary connecting it to the Peter the Great Bay, featuring a semi-circular area with a radius $L \approx 14$ km and a depth at the entrance $H \approx 50$ m. For such marine areas, a pronounced occurrence of the longitudinal zero-mode of eigenoscillations is typical, where a quarter-wavelength fits within the area, and the nodal line is located near its entrance. The calculated period of this so-called fundamental, or zero, SO mode in a marine area with parameters similar to those of the Posyet Bay is ~ 47 minutes. The periods of subsequent modes are close to the spectral maximum periods at frequencies of $\nu_1 \approx 1/33$, $\nu_2 \approx 1/27$, $\nu_3 \approx 1/22$ min^{-1} .

A study of the mutual influence of two adjacent inlets on each other during resonant response in [12] showed that the presence of an adjacent inlet leads to an intensification of the zero (fundamental) mode in both inlets. Since the Peter

the Great Bay includes, besides the Posyet Bay, also the Amursky and Ussuriysky gulfs, each of them influences sea level fluctuations in the neighboring waters. In this regard, periods of the zero mode for the Amursky and Ussuriysky gulfs, using the simplest analytical models of these gulfs, will be estimated.

The Amursky Gulf has a shape close to a rectangle with a length of 50 to 60 km and a depth at the entrance from 45 to 50 m. Assuming the bottom profile of the gulf has a linear dependence, the period of the fundamental longitudinal mode in such a gulf will range from 200 to 240 minutes. Let us define the shape of the Ussuriysky Gulf's area boundary as an irregular isosceles triangle with a length from the mouth to the apex of $L \sim 40\text{--}50$ km, a depth at the entrance from 50 to 70 m, and a quadratic bottom profile. In such a gulf, the period of the fundamental longitudinal mode would range from 130 to 140 minutes, and the period of the first mode from 90 to 94 minutes.

Sea level fluctuations induced by shelf seiches in the Posyet Bay

As is known, the surface wave field in bays, inlets, and the adjacent shelf area is formed both by eigenoscillations and by oscillations of the continuous spectrum of waves radiated by the shelf. According to research, waves propagating from the open sea (Poincaré waves), as a result of multiple reflections from the coast and the shelf edge, can be significantly amplified at selected resonant frequencies. Thus, the superposition of the incoming Poincaré wave and the wave reflected from the coast leads to the excitation of standing sea level oscillations with periods corresponding to so-called shelf seiches⁴.

To describe the continuous spectrum of Poincaré waves, the amplitude amplification coefficient γ is used – the ratio of the wave amplitude at the coast to its amplitude in the open sea. This coefficient depends on frequency ω , the alongshore wavenumber k , and the shelf bathymetry. In essence, the function $\gamma(\omega, k)$ can be interpreted as the transfer function of the open sea–coast system. Therefore, at frequencies where this function has maxima (i.e., at resonant frequencies), corresponding maxima can be expected in the spectra of sea level fluctuations.

For a shelf with bathymetry defined by the simplest expression below

$$h(x) = \begin{cases} \alpha x & \text{when } 0 < x < L, \\ H & \text{when } x > L, \end{cases}$$

the amplification coefficient takes the following form

$$\gamma(\omega) = \left[J_0^2(\sigma) + d J_1^2(\sigma) \right]^{-1/2}, \quad (1)$$

where $\sigma = \lambda\sqrt{L}$, $\lambda = \sqrt{L(\omega^2 - f^2)} / \sqrt{gh}$, $h = \alpha L$, $d = h/L$.

⁴ Yefimov, V.V., Kulikov, E.A., Rabinovich, A.B. and Fine, I.V., 1985. [*Ocean Boundary Waves*]. Leningrad: Gidrometeoizdat, 280 p. (in Russian).

Let us consider a model shelf with parameters: $f = \frac{2\pi}{17.7}$ rad/h, $h = 201$ m, $L = 35$ km and $H = 4$ km, similar to the corresponding parameters of the shelf in the bay area. According to relation (1), the amplification coefficient γ for radiated waves on such a shelf has maxima at periods of 178, 134, 107, and 90 minutes. These values show good agreement with the maxima in the sea level fluctuation spectrum (see Figs. 2 and 3). Thus, the listed spectral maxima at the indicated periods are most likely formed by radiated waves due to shelf resonance between the incident and reflected Poincaré waves.

Let us proceed to interpreting the features of the sea level fluctuation spectrum in the bay, based on the assumption that these oscillations are generated by seiches as well as radiated waves over the shelf adjacent to the bay. Using a model bay with parameters close to those of the bay, the periods of its zero ($T_0 \sim 47$ min) and subsequent ($T_1 \sim 33$, $T_2 \sim 26$, $T_3 \sim 23$ min) seiche oscillation modes were calculated. As can be seen, the obtained values correspond to the positions of maxima in the high-frequency part of the spectrum (see Fig. 2, *b*).

Another important source of sea level fluctuations is radiated waves generated by Poincaré waves. Over the shelf ~ 38 km wide, with a slope to the depth at its seaward edge (~ 4 km), these waves form standing sea level fluctuations with periods of $T_1 \sim 178$ min, $T_2 \sim 134$ min, $T_3 \sim 107$ min, and ~ 90 min. The obtained model periods correspond to the positions of maxima in the observed sea level fluctuation spectra (Fig. 3).

Spectral composition of temperature fluctuations and bottom pressure in the study area

Let us turn to the coastal water temperature measurement data obtained during the experiment. Spectral analysis of the original time series was performed for two temporal scales (Fig. 4). In the submesoscale range (6-minute sampling interval), the spectrum (Fig. 4, *a*) is characterized by maxima at periods of 205, 170, 135, 107, 94, and 70 minutes, which correspond to the peaks previously identified in the sea level fluctuation spectrum. In the mesoscale range (30-minute sampling interval), maxima are observed at periods of 12.6, 17.1, 38.0, 7.0, and 6.3 hours (Fig. 4, *b*).

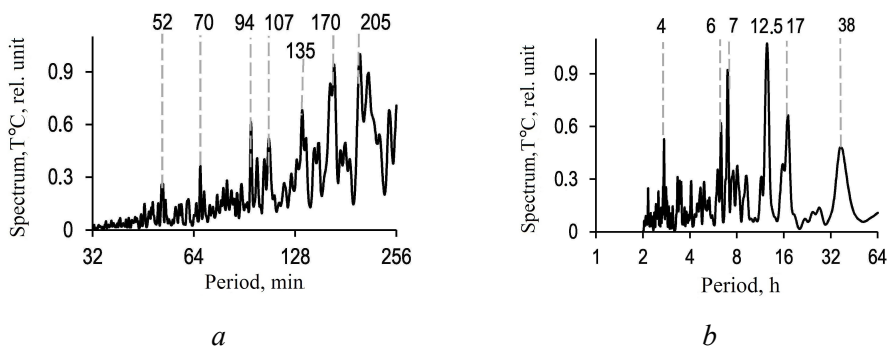


Fig. 4. Spectrum of temperature pulsations in the ranges $1/32$ – $1/256$ min^{-1} (*a*) and 1 – $1/64$ min^{-1} (*b*)

The interpretation of the spectral features of temperature fluctuations in the mesoscale range should consider the dynamics of baroclinic disturbances in the coastal zone of marginal seas. It has been established that such disturbances are caused by barotropic tidal or inertial flow [13]. Their interaction with the continental slope generates significant vertical movements of large seawater masses, creating a “mass force” – a source of baroclinic disturbances evolving into IGWs with tidal or inertial frequencies. The spectral signature of this “mass force” confirms the mixed character of the barotropic tide in the bay, with diurnal constituents predominating.

Baroclinic disturbances can be conditionally divided into forced IGWs with frequencies of the barotropic tide and spatial scales determined by inhomogeneities of bottom topography in the generation zone, and free IGWs whose spatiotemporal scales are determined by the environmental properties through the dispersion relation, and whose temporal scales are limited by the region of existence for this type of wave motion:

$$f < \omega < N_{\max},$$

where N_{\max} is the maximum value of the Väisälä–Brunt frequency in the study area during the considered time period.

The interpretation of mesoscale variability of hydrological parameters will continue using a model of a stratified fluid perturbed by an IGW field. According to [14], internal waves represent small deviations of hydrophysical parameters from their equilibrium values. For example, temperature variations δT are related to the wave field by the expression

$$\delta T = i\omega\eta \cdot (d \langle T_0(z) \rangle / dz),$$

where $\langle T_0(z) \rangle$ is the background temperature distribution; η is the vertical displacement of “fluid particles” with frequency ω in the wave field. The displacement η in a stratified fluid can be represented as a superposition of normal modes of internal waves:

$$\zeta = \sum A_n \cdot \psi_n(z) \cdot \exp[i(k_x x + k_y y - \omega t)],$$

where $k = \sqrt{k_x^2 + k_y^2}$ is the horizontal wavenumber vector; $\psi_n(z)$ is the amplitude function of the IGW mode with number n . Under the Boussinesq approximation, the set of these functions forms a solution to the eigenvalue boundary problem:

$$\frac{d^2 \psi_n}{dz^2} + k^2 \frac{N^2 - \omega^2}{\omega^2 - f^2} \psi_n = 0, \quad (2)$$

with the boundary “solid lid” conditions

$$\psi_n = 0 \text{ при } z = 0 \text{ и } z = -H. \quad (3)$$

Let us write the expression for pressure fluctuations created by the n -th mode of the IGW:

$$p_n = -iC_n \cdot (\omega^2 - f^2) k^{-2} \omega^{-1} (\rho_0 d\psi_n(z)/dz) \cdot \exp\left[i(k_x x + k_y y - \omega t)\right]. \quad (4)$$

According to formula (4), the pressure created by an IGW with frequency $\omega \rightarrow f$ approaches zero; that is, any IGW mode with such frequencies creates negligibly small pressure in the bottom layer. In other words, the proximity of bottom pressure to zero is a characteristic feature of a coastal IGW with a frequency close to f , or an internal Kelvin wave.

Let us now proceed to the analysis and interpretation of coastal water temperature variability in the bay caused by the IGW field. The absence of a spectral maximum at a frequency of $1/24 \text{ h}^{-1}$ is explained by the fact that this frequency lies beyond the existence boundary for IGWs. The peak at a frequency of $\sim 1/12 \text{ h}^{-1}$ is commonly observed in ocean parameter spectra and indicates the transfer of energy from the semidiurnal tide into internal waves [15]. At the same time, the peak in the seawater temperature fluctuation spectrum at the semidiurnal frequency in the area of the SBS deployment corresponds to forced waves.

The maxima in the spectrum at periods of 17, 16, and 38 hours can be interpreted as a occurrence of internal Kelvin waves (KIWs), which are formed near the steep coast of the Gamov Peninsula (see Fig. 1) [16, 17]. In a right-handed coordinate system where the Ox axis is directed along the coast, the Oy axis is directed away from the coast, and the Oz axis is directed vertically upward, the parameters of KIWs, which propagate along the coastal boundary and decay exponentially with normal distance from the shore, have the following form:

$$w = \sum_m C_m \psi_m(z) \exp\left[-f y/c_m + ik_m(x - c_m t)\right]$$

and they can be determined by solving the boundary value problem for eigenvalues:

$$d^2 \psi_m / dz^2 + N^2 c_m^{-2} \psi_m = 0, \quad (5)$$

$$\psi_m = 0 \text{ when } z = 0 \text{ and } z = -H, \quad (6)$$

where c_m is the phase velocity of the KIW with mode number m . From relation (5) it follows: (a) the phase velocity of this wave is independent of its frequency, i.e., KIWs are non-dispersive; (b) at $\omega \cong f$, the boundary value problem in (5) and (6) lacks the singularity present in the boundary value problem in (2) and (3). Consequently, a KIW with the inertial frequency f generates a bottom pressure that, in the presence of a pycnocline in the bottom layers, reaches its maximum value.

Analysis of the boundary value problem (5) and (6) shows that for a fixed frequency ω , the KIW field is characterized by a discrete set of amplitude functions $\{\psi_m\}$ and a corresponding set of phase velocities $\{c_m\}$ or wavenumbers $\{k_m = \omega/c_m\}$. All these wave field parameters can be found by solving the eigenvalue boundary value problem (5) and (6). Its solution is determined by the depth distribution of the parameter $N(z)$. However, in the observation area, the presence of

a coastal background current is possible, which can lead to advective transport of the wave field relative to the sensors. Spectra obtained from such data are characterized by a distribution of wave oscillation energy not over the true frequencies ω , but over Doppler-shifted frequencies: $\omega_D = \omega \pm kU_0$. It is known [18, 19] that, propagating in a background flow, a normal IGW mode with number n will induce oscillations of hydrophysical parameters with a frequency ω_n , different from the frequency ω in still water. In the case of an alongshore background flow with velocity U_0 these two frequencies, or periods, are related by the Doppler relation:

$$T_m = T (1 - U_0/c_m). \quad (7)$$

In this expression, the “minus” sign is chosen based on the assumption that the waves propagate from the seaward zone of the bay along the coastal background flow directed into its inner part.

Thus, the m -th KIW mode with period m and $T_i = 1/f$, where f is the inertial frequency, propagating in the coastal flow of the bay, induces oscillations of hydrophysical parameters with various periods $\{T_m\}$, which are related to the inertial period $T_i = T$ by relation (7). It is highly probable that in 2009, hydrological conditions similar to those in 2005 developed in the coastal zone of the Gamov Peninsula.

The buoyancy frequency profile $N(z)$ characteristic of September 2009, taken from [20] and presented in Fig. 5, *a*, indicates an autumn type of density stratification with a pycnocline shifted towards the bottom layer.

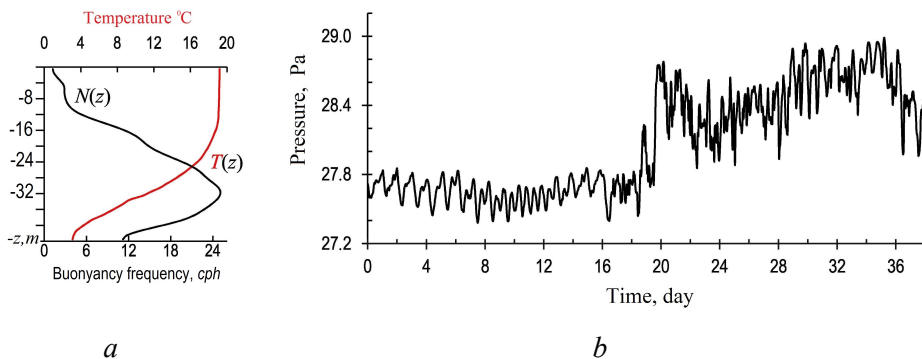


Fig. 5. Typical profiles of temperature T and buoyancy frequency $N(z)$ (*a*), and bottom pressure record (*b*) in the observation area

Another feature of the spectrum in Fig. 4, *a* is related to the presence of a maximum at a period of ~ 6.3 h. It was previously established that KIWs in the coastal zone of the Gamov Peninsula exhibit nonlinear properties [21]. In other words, during their evolution, the shape of the KIWs becomes increasingly asymmetric. The rear front becomes steeper, while the leading front becomes more gentle. Harmonics of the carrier frequency $1/12.4 \text{ h}^{-1}$, i.e., frequencies of $\sim 1/6$ and

$\sim 1/4 \text{ h}^{-1}$, appear in the wave field spectrum, the first of which is recorded in the spectrum in Fig. 4, *b*.

Let us analyze the measurement data of bottom pressure fluctuations in the coastal waters recorded during the experiment. Hydrostatic pressure measurements were taken every second in centimeters of mercury. The data were then converted into centimeters of water column and averaged over a 60-second interval using the weighting coefficients of the Kaiser–Bessel filter (to suppress the potential influence of wind waves, which can occur when using a standard rectangular window). The time series of pressure fluctuations in the area of the pressure sensor deployment, obtained over 38 days (from 28.08.2009 to 14.10.2009), shows an abrupt change in spectral composition on the 16th day of observations (Fig. 5, *b*), which lasted about three weeks.

During the first 16 days, the device recorded pressure fluctuations caused by tidal sea level oscillations. According to measurements in the bay, the tide is of a mixed type with a slight predominance of the diurnal harmonic. The spectrum of these oscillations confirms this (Fig. 6, *a*). As shown in the figure, the spectrum is formed by two prominent maxima at the semidiurnal and diurnal frequencies: $\sim 1/12.4$ and $\sim 1/25.6 \text{ h}^{-1}$, respectively.

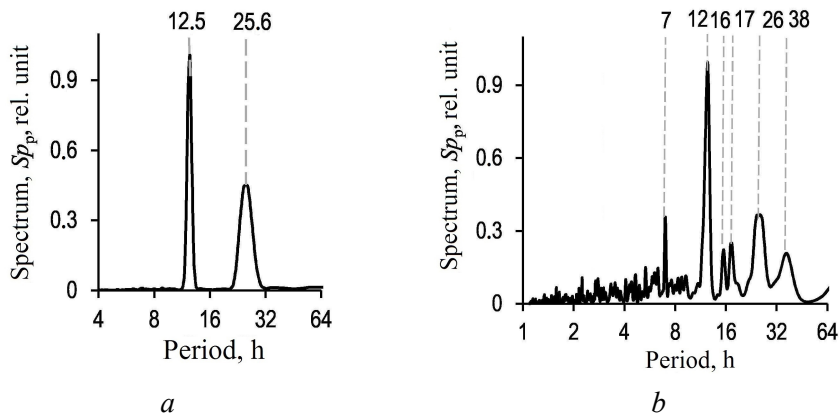


Fig. 6. Spectra of pressure pulsations in the first two weeks (*a*) and in the following three weeks (*b*)

Let us consider the spectral composition of pressure fluctuations from the second half of the time series L_2 (Fig. 6, *b*). A comparison of the two spectra (Fig. 6) shows that both contain maxima at frequencies of $\sim 1/12.4$ and $\sim 1/26 \text{ h}^{-1}$, formed by tidal sea level oscillations. However, the spectrum of series L_2 additionally contains maxima at frequencies of $1/7$, $1/16$, $1/17$, and $1/38 \text{ h}^{-1}$.

It is highly probable that the reason for these differences between the two spectra is the baroclinicity of the bay's coastal waters. It is known that pressure fluctuations in the coastal sea zone consist of barotropic and baroclinic components. The barotropic component corresponds to tidal sea level oscillations, while mesoscale temperature oscillations are of baroclinic origin. After removing

the barotropic component, the spectrum of residual baroclinic pressure fluctuations was obtained (Fig. 7, *b, c*).

Its main difference from the spectrum in Fig. 7, *a* is the absence of a maximum at the frequency $\sim 1/25.6 \text{ h}^{-1}$ (Fig. 7, *b*), meaning that pressure fluctuations at the frequency of diurnal tidal oscillations are absent. As is known, the internal tide in the Peter the Great Bay possesses a similar feature: this wave process can only exist under conditions of density stratification (baroclinicity) of coastal waters. Residual bottom pressure fluctuations at the $1/12.4 \text{ h}^{-1}$ frequency also indicate their baroclinic nature, and the spectrum of these fluctuations represents the spectrum of pressure fluctuations generated by internal waves. Another confirmation of this assumption can be the significant similarity between the spectra of temperature fluctuations caused by IGWs and the spectrum of the baroclinic component of bottom pressure fluctuations.

Another feature of the spectrum in Fig. 7 is that the oscillation periods of 16 and 17 h, where its maxima are located, are close to the inertial period $T_i = 1/f$, where $f = 2\Omega |\sin\phi|$ is the Coriolis parameter at the observation latitude ϕ . The latitude of the observations is $\phi \sim 42^\circ 35'$. Thus, the period T_i is 17.7 h. Furthermore, as follows from Fig. 7, fluctuations at periods close to T_i , have a duplet structure, associated with the maximum at a period of 16 h. The interpretation for the formation of this structure is given in the text above and is attributed to the coastal background flow directed into the inner part of the bay.

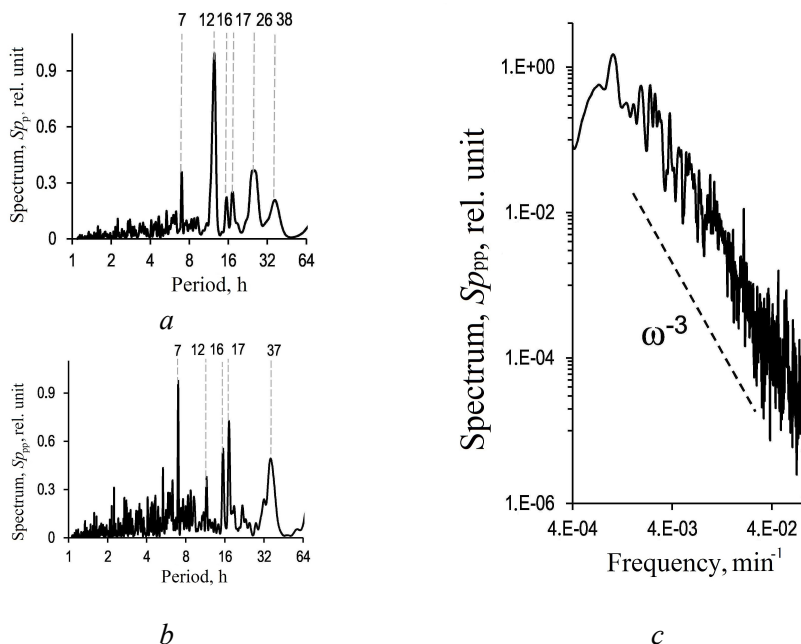


Fig. 7. Pulsation spectra of the barotropic (*a*) and baroclinic (*b* by period, *c* by frequency) components of bottom pressure

And finally, the spectrum draws attention to a narrowband maximum of clearly resonant nature at a frequency of $1/7 \text{ h}^{-1}$, the origin of which requires further study. It should only be noted that the sum of frequencies $1/12.4$ and $1/17.7 \text{ h}^{-1}$ is close to $1/7 \text{ h}^{-1}$, and their difference is close to $1/38.4 \text{ h}^{-1}$, which indicates possible nonlinear interaction of internal waves.

The results of the presented analysis indicate the similarity between the spectrum of temperature fluctuations in the pycnocline and the spectrum of the baroclinic component of bottom pressure. In [22], it was suggested that the existence of KIWs in the coastal zone of the Gamov Peninsula is possible. A specific feature of these waves is intense pressure fluctuations at frequencies close to the inertial frequency. It is precisely this feature of the pressure fluctuation spectrum that was recorded by the pressure sensor. Therefore, the recorded pressure fluctuations and their corresponding spectrum are formed by KIWs. Thus, another possibility for recording KIWs opens up, alongside measuring vertical particle displacements by recording the baroclinic component of pressure fluctuations.

In the high-frequency part of the baroclinic pressure spectrum (range $4.0\text{E-}04 - 4.0\text{E-}02 \text{ min}^{-1}$), its character changes from discrete (narrow peaks in Fig. 7, *a, b*) to continuous, and the energy decay follows a law close to $\sim \omega^{-3}$ (Fig. 7, *c*). This asymptote differs from the canonical spectrum of linear internal waves ω^{-2} [23]. However, it has been recorded in studies of nonlinear internal waves [24, 25], where it is associated with the process of wave field evolution: growth of wave asymmetry, generation of harmonics of the carrier frequency, and their subsequent nonlinear interaction leading to the formation of a frequency continuum. This is consistent with data on the occurrence of nonlinear properties of IGWs in the Posyet Bay, leading to harmonic generation and the formation of a spectrum with ω^{-3} asymptotics.

Conclusion

Based on the analysis of observational time series, the variability of sea level, temperature, and bottom pressure in the coastal waters of the Posyet Bay was studied. It was established that submesoscale sea level variability (periods $\sim 18, \sim 22, \sim 25, \dots, \sim 47, \sim 94, \sim 107, \dots, \sim 205 \text{ min}$) is formed by resonant processes: the zero and higher modes of eigen (seiche) oscillations of the model area approximating the bay, as well as by shelf seiches excited by radiated Poincaré waves over the adjacent slope. Spectra of submesoscale temperature fluctuations and the baroclinic component of bottom pressure demonstrate a spectral structure similar to that of sea level, indicating their common topographic origin.

Mesoscale variability of hydrological parameters is determined by wave impacts (M_2 harmonics) and atmospheric forcing (quasi-inertial oscillations). The key features of the baroclinic pressure spectrum are: a) the absence of a maximum at the diurnal tidal frequency ($\sim 1/25.6 \text{ h}^{-1}$); b) the presence of narrowband maxima at frequencies close to the inertial frequency ($\sim 1/16$ and $1/17 \text{ h}^{-1}$).

It is shown that these features are associated with the generation and propagation of KIWs. The presence of maxima in the bottom pressure spectrum is interpreted as a result of the Doppler shift of the KIW frequency in the bottom coastal flow

directed into the inner part of the bay. This confirms the effectiveness of the method of recording the baroclinic component of bottom pressure for detecting this type of wave.

During the evolution of the wave field, harmonics of the inertial frequency appear in its spectrum, i.e., its non-stationarity increases. Further interaction of the harmonics forms a continuous frequency dependence in the spectrum (frequency continuum) with an asymptote of the form ω^{-3} . Such an asymptote is documented for the first time for the spectrum of fluctuations of the baroclinic component of bottom pressure in the coastal waters of the Posyet Bay in the presented article.

To clarify the mechanisms for the formation of a similar structure in the submesoscale sea level, bottom pressure, and coastal water temperature oscillations in the Posyet Bay, as well as the cause and mechanism for the formation of the resonant peak at frequency $\sim 1/7 \text{ h}^{-1}$ and the broadband maximum at frequency $\sim 1/40 \text{ h}^{-1}$, further research is necessary.

REFERENCES

1. Wilson, B.W., 1972. Seiches. In: V. T. Chow, ed., 1972. *Advances in Hydrosience*. New York: Academic Press. Vol. 8, pp. 1-94. <https://doi.org/10.1016/B978-0-12-021808-0.50006-1>
2. Rabinovich, A.B., 2009. Seiches and Harbor Oscillations. In: Y. C. Kim, ed., 2009. *Handbook of Coastal and Ocean Engineering*. Singapore: World Scientific Publishing, pp. 193-236. https://doi.org/10.1142/9789812819307_0009
3. Miropol'sky, Yu.Z., 2001. *Dynamics of Internal Gravity Waves in the Ocean*. Atmospheric and Oceanographic Sciences Library; vol. 24. Dordrecht: Springer, 406 p.
4. Lemmin, U., 2012. Internal Seiches. In: L. Bengtsson, R. W. Herschy and R. W. Fairbridge, eds., 2012. *Encyclopedia of Lakes and Reservoirs*. Encyclopedia of Earth Sciences Series. Dordrecht: Springer, pp. 410-414. https://doi.org/10.1007/978-1-4020-4410-6_160
5. Volkov, S.Yu., Bogdanov, S.R., Zdorovenov, R.E., Palshin, N.I., Zdorovenova, G.E., Efremova, T.V., Gavrilenko, G.G. and Terzhevnik, A.Yu., 2020. Resonance Generation of Short Internal Waves by the Barotropic Seiches in an Ice-Covered Shallow Lake. *Physical Oceanography*, 27(4), pp. 374-389. <https://doi.org/10.22449/1573-160X-2020-4-374-389>
6. Rabinovich, A.B., 1993. *Long Gravitational Waves in the Ocean: Capture, Resonance, and Radiation*. Saint Petersburg: Gidrometeoizdat, 325 p. (in Russian).
7. Dolgikh, G.I., Budrin, S.S., Dolgikh, S.G., Plotnikov, A.A., Chupin, V.A., Shvets, V.A. and Yakovenko, S.V., 2016. Free Oscillations of Water Level in the Posyet Gulf Bays (the Sea of Japan). *Russian Meteorology and Hydrology*, 41(8), pp. 559-563. <https://doi.org/10.3103/S1068373916080057>
8. Chupin, V., Dolgikh, G., Dolgikh, S. and Smirnov, S., 2022. Study of Free Oscillations of Bays in the Northwestern Part of Posyet Bay. *Journal of Marine Science and Engineering*, 10(8), 1005. <https://doi.org/10.3390/jmse10081005>
9. Smirnov, S.V., Yaroshchuk, I.O., Leontyev, A.P., Shvyrev, A.N., Pivovarov, A.A. and Samchenko, A.N., 2018. Studying Resonance Oscillations in the Eastern Part of the Posyet Bay. *Russian Meteorology and Hydrology*, 43(2), pp. 88-94. <https://doi.org/10.3103/S1068373918020048>
10. Emery, W.J. and Thomson, R.E., 2001. *Data Analysis Methods in Physical Oceanography*. Amsterdam, Netherlands: Elsevier Science, 654 p.
11. Novotryasov, V.V., 2024. Excitation of Internal Waves in a Shallow Sea Basin with an Open Inlet under Conditions of Parametric Resonance. *Physical Oceanography*, 31(5), pp. 647-661.

12. Manilyuk, Yu.V., Lazorenko, D.I. and Fomin, V.V., 2019. Resonance Oscillations in the System of Adjacent Bays. *Physical Oceanography*, 26(5), pp. 374-386. <https://doi.org/10.22449/1573-160X-2019-5-374-386>
13. Baines, P.G., 1982. On Internal Tide Generation Models. *Deep-Sea Research Part A. Oceanographic Research Papers*, 29(3), pp. 307-338. [https://doi.org/10.1016/0198-0149\(82\)90098-X](https://doi.org/10.1016/0198-0149(82)90098-X)
14. Konyayev, K.V. and Sabinin, K.D., 1992. [*Waves in the Ocean*]. Saint Petersburg: Gidrometeoizdat, 272 p. (in Russian).
15. Munk, W. and Wunsch, C., 1998. Abyssal Recipes II: Energetics of Tidal and Wind Mixing. *Deep-Sea Research Part I: Oceanographic Research Papers*, 45(12), pp. 1977-2010. [https://doi.org/10.1016/S0967-0637\(98\)00070-3](https://doi.org/10.1016/S0967-0637(98)00070-3)
16. LeBlond, P.H. and Mysak, L.A., 1978. *Waves in the Ocean*. Elsevier Oceanography Series; vol. 20. Amsterdam: Elsevier Scientific Publishing Company, 602 p. [https://doi.org/10.1016/S0422-9894\(08\)X7037-0](https://doi.org/10.1016/S0422-9894(08)X7037-0)
17. Gill, A.E. and Clarke, A.J., 1974. Wind-Induced Upwelling, Coastal Currents and Sea-Level Changes. *Deep-Sea Research and Oceanographic Abstracts*, 21(5), pp. 325-345. [https://doi.org/10.1016/0011-7471\(74\)90038-2](https://doi.org/10.1016/0011-7471(74)90038-2)
18. White, W.B., 1972. Doppler Shift in the Frequency of Inertial Waves Observed in Moored Spectra. *Deep Sea Research and Oceanographic Abstracts*, 19(8), pp. 595-600. [https://doi.org/10.1016/0011-7471\(72\)90042-3](https://doi.org/10.1016/0011-7471(72)90042-3)
19. Gerkema, T., Maas, L.R.M. and van Haren, H., 2013. A Note on the Role of Mean Flows in Doppler-Shifted Frequencies. *Journal of Physical Oceanography*, 43(2), pp. 432-441. <https://doi.org/10.1175/JPO-D-12-090.1>
20. Novotryasov, V.V. and Vanin, N.S., 2002. Low-Frequency Internal Waves in the Near-Shore Zone of the Japan Sea. *Izvestiya AN. Fizika Atmosfery i Okeana*, 38(4), pp. 557-565 (in Russian).
21. Novotryasov, V.V., Vanin, N.S. and Karnaukhov, A.A., 2005. Manifestation of Nonlinear Properties of Internal Kelvin Waves in the Coastal Zone of the Sea of Japan. *Izvestiya, Atmospheric and Oceanic Physics*, 41(5), pp. 611-619.
22. Novotryasov, V.V. and Karnaukhov, A.A., 2009. Nonlinear Interaction of Internal Waves in the Coastal Zone of the Sea of Japan. *Izvestiya, Atmospheric and Oceanic Physics*, 45(2), pp. 262-270. <https://doi.org/10.1134/S000143380902011X>
23. Garrett, C. and Munk, W., 1972. Space-Time Scales of Internal Waves. *Geophysical Fluid Dynamics*, 3(3), pp. 225-264. <https://doi.org/10.1080/03091927208236082>
24. Van Haren, H., 2004. Some Observations of Nonlinearly Modified Internal Wave Spectra. *Journal of Geophysical Research: Oceans*, 109(C3), C03045. <https://doi.org/10.1029/2003JC002136>
25. Filonov, E.A. and Lavín, M.F., 2003. Internal Tides in the Northern Gulf of California. *Journal of Geophysical Research: Oceans*, 108(C5), 3151. <https://doi.org/10.1029/2002JC001460>

Submitted 20.05.2025; approved after review 20.06.2025;
accepted for publication 10.11.2025.

About the authors:

Vadim V. Novotryasov, Leading Researcher of the Department of Ocean & Atmosphere Physics, V. I. Il'ichev Pacific Oceanological Institute, Far Eastern Branch of Russian Academy of Sciences (43 Baltiyskaya Str., Vladivostok, 690041, Russian Federation), DSc. (Phys.-Math.), Associate Professor, **ORCID ID: 0000-0003-2607-9290**, **SPIN-code: 4584-8071**, vadimnov@poi.dvo.ru

Georgiy V. Shevchenko, Head of the Oceanography Laboratory, Sakhalin Branch of the All-Russian Research Institute of Fisheries and Oceanography (VNIRO) (196 Komsomolskaya Str., Yuzhno-Sakhalinsk, 693023, Russian Federation); Leading Researcher of the Tsunami Laboratory, Institute of Marine Geology and Geophysics, Far Eastern Branch of the Russian Academy of Sciences (1B Nauki Str., Yuzhno-Sakhalinsk, 693023, Russian Federation); DSc. (Phys.-Math.), **ORCID ID: 0000-0003-0785-4618**, **SPIN-code: 8230-2974**, shevchenko_zhora@mail.ru

Contribution of the co-authors:

Vadim V. Novotryasov – conceptualization, data curation, formal analysis, visualization, writing of original draft, review and editing

Georgiy V. Shevchenko – investigation, resources, data curation, formal analysis, writing of original draft, review and editing

The authors have read and approved the final manuscript.

The authors declare that they have no conflict of interest.